Characteristics of Red Clay of Douglas County, Wisconsin

BRUCE E. BROWN AND J.T. MENGEL

In the red clay region of Douglas County, Wisconsin, three types of stratigraphic succession are observed from borehole data: red clay 8 m (25 ft) thick over older red clay, red clay over brown or gray clay, and red clay over brown sand. The mean contents with standard deviation of sand (>44 μm), silt (44 to 2 μm), coarse clay (2 to 0.2 μm), and fine clay (<0.2 μm) in red clay from 28 borehole samples are 4 ± 4, 24 ± 12, 42 ± 7, and 30 ± 6. Smectite clay is dominant in the fine clay fraction; illite and chlorite are dominant in the coarse clays; and quartz, feldspars, and carbonates are dominant in the silt and sand fractions. Particle-size distribution and mineral contents correlate with the Atterberg limit values. The equations Liquid limit = 10.0 + 0.78 (% <2 μm clay) and Plasticity index = -0.1 + 0.51 (% <2 μm clay) have correlation coefficients of 0.76 and 0.84, respectively, for this body of data. The dominant failure mode in the Little Balsam Creek drainage south of Superior and in other similar locales involves drying and cracking of a surficial layer of clay that then slides as a decollement sheet over the underlying clay. This failure may have been promoted by recent cultural practice in the area.

Along the shore of Lake Superior from Michigan to the Minnesota border, is an extensive area of red-brown clay-rich sediments that have locally been dubbed the "red clay." The focus of this paper is on the characteristics of this material in Douglas County, Wisconsin. As the observed properties of the red clay are roughly similar throughout Douglas County, it is probable that the characteristics described here will be found throughout the red clay region. The red clay underlies the gently sloping Superior plain that, in Douglas County, ranges from about 190 m (625 ft) above mean sea level along the lake to about 335 m (1,100 ft) along the South Range, a sand-covered highland with a lava bedrock core. The South Range is the south boundary of the red clay region (see Figure 1). The red clay is glacially derived and consists of a thick surface layer of red-brown and associated grayish clays and brown sands. It rests on a vaguely stratified clay layer that contains large, but variable, amounts of silt, sand, gravel, and coarser material. These Quaternary age sediments are underlain, in turn, by red sandstones or black basaltic lava flows of late Precambrian (Keweenawan) age.

Figure 1. The area occupied by the red clay in Douglas County, Wisconsin.

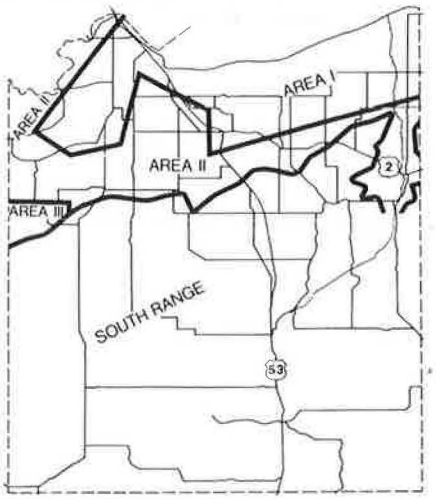

DOUGLAS COUNTY
SLOPE STABILITY TYPE AREAS

STRATIGRAPHIC SUCCESSION

The Quaternary age sediments accumulated at a time when the last continental glacier to cover the region was retreating but still filled the eastern end of the Lake Superior basin, impounding high level lakes in the western end (1). The floor of these lakes, now the surface of the plain, is dissected by a drainage system that is still in a geologically youthful stage of evolution and undergoing the kind of valley deepening and widening characteristic of such a stage.

In Little Balsam Creek drainage, south of the 320-m (1,050-ft) topographic contour, the stratigraphic succession within about 9 m of the upland surface is a clean, fine- to medium-grained brown sand containing small amounts of gravel and rare boulders. A similar sand is present along the South Range across the county. The sands are above the level of strong lake action and exhibit a knob and kettle or channeled outwash topography that contrasts sharply with the smooth upland surface of the red clay plain below an elevation of 335 m. In the Little Balsam area and elsewhere, the sand grades laterally into the clay of the plain within a short distance.

North of the 320-m contour, in the Little Balsam drainage, the gently rolling upland surface of the plain is underlain by a red-brown clay layer that can be up to 8 m thick. Beneath this layer the succession may include one of three other layers: (a) a second, older red clay; (b) brownish-gray or grayish-brown clays that show varves in some outcrops (SW1/4 sec. 34, T. 47 N., R. 15 W., for example); and (c) a fine- to medium-grained brown sand. The sands and varved clays may represent a time of temporary ice retreat between the times of ice advance recorded by the two red clays. The top of the older red clay layer shows markedly higher resistance to indentation by a simple spring penetrometer (2 to 3 TSf) than does the varved clay or basal part of the younger red clay (0.4 to 1.5 TSf). (Such resistance measurements were made as auger flights were removed from the drill hole.)

Figure 1 shows the portions of the red clay area underlain by each type of stratigraphic succession. Area I, including the coastal townships, much of Superior, and the area south of the city, is underlain by two red clays having little other material between. Area II, the St. Louis River valley and the higher elevation adjacent to the South Range, is the portion of the red clay area where upper and lower red clay layers are separated by considerable thicknesses of sand. Area III includes portions of the red clay where the varved clays occur between the two red clays.

NATURE OF RED CLAY MATERIAL

Samples from a number of representative boreholes (Figure 2) were used to determine particle-size distribution, mineral content, and Atterberg limit values.

Particle-Size Distribution in Red Clay

Samples were separated into sand (>44 μm), silt (44 to 2 μm), coarse clay (2 to 0.2 μm), and fine clay (<0.2 μm) separates using a centrifuge washing procedure after Jackson (2); dispersion was first accomplished using iron oxide removal (3) and sodium hexametaphosphate dispersant (0.5 percent). Two triangular diagrams (see Figures 3 and 4) are plotted from the observed distributions. Figure 3 (sand, silt, clay) shows this material to range from clay to silty clay with sand contents typically below 10 percent. Figure 4 (silt, coarse clay, fine clay) shows a relatively uniform ratio of coarse clay to fine clay of about 60/40 with greater variation in silt contents.

Figure 2. Locations of boreholes from which red clay samples were taken.

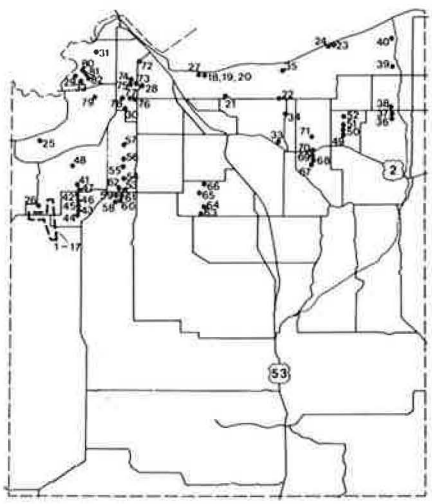

Mineralogy of Red Clay

Both nonlayer silicate minerals (quartz, feldspars, dolomite, calcite) and layer silicate clays were determined on the silt, coarse clay, and fine clay separates. The amounts of nonlayer silicate minerals were determined using an internal standard X-ray method.

For quartz, calcite, and dolomite, it was possible to prepare standard mixtures with an alpha-alumina (corundum) internal standard. The results for these three minerals are thought to be reliable to within ±5 percent. No adequate primary standards are available for the feldspars in these samples. Using relative line intensities it was possible to achieve good relative values for the feldspars from sample to sample, but the absolute amounts are estimates only. From this procedure, an estimate of the total clay mineral content can be derived by difference (i.e., 100 - percentage quartz + percentage calcite + percentage dolomite + percentage feldspars). Three major clay species were identified in all of the red clay samples. Smectite (montmorillonite) is indicated by the presence of a line near 18A on glycolated samples, chlorite by the presence of a heatstable 14A line plus subsidiary orders, and illite by the presence of a line at 10A plus subsidiary orders. Interstratified clays were present but minor and kaolinite, also minor, was not easily identified because of the presence of chlorite. To accurately determine the amounts of smectite it is necessary to carry out size separations. Whole-sample X-raying underestimates smectite and results in less consistent data.

Clay mineral percentages were derived from X-ray peak intensities using scale factors appropriate to the clay species and normalizing sums to 100 percent. Table 1 gives a summary of mineral content data. Triangular diagrams (Figures 5 and 6) summarize the proportions of clay versus nonclay minerals in the red clay and the proportions of illite to chlorite to smectite in the fine clay (where no nonclay minerals are detected).

Figure 6 shows smectite as the most variable component of the fine clay fraction. There is a rela-

Figure 3. Sand, silt, and clay contents for red clay samples taken from boreholes 12, 18, 21-33, 35, 36, 38-40, 42, 72, 74, 75, 77, and 79-82.

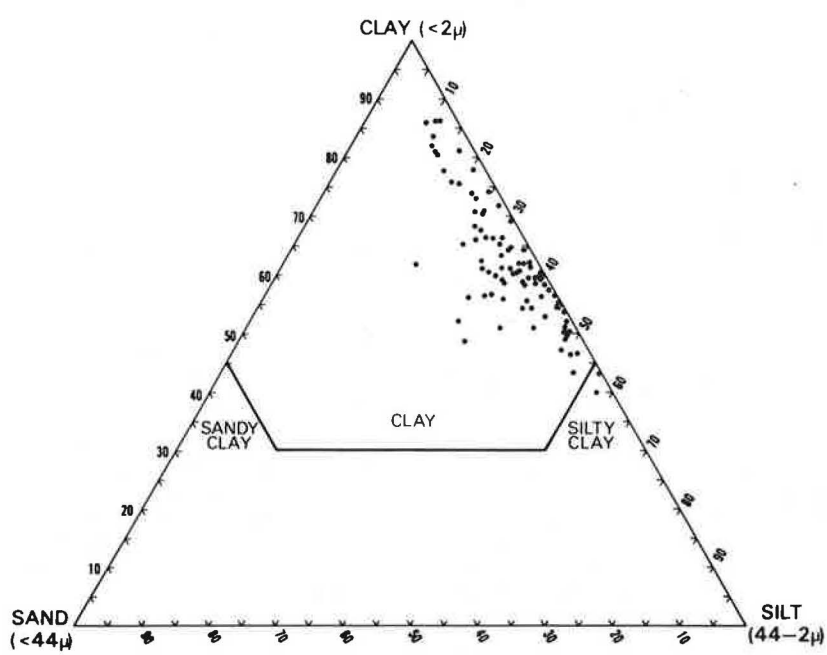

Figure 4. Silt, coarse clay, and fine clay contents for the red clay from boreholes 12, 18, 21, 22, 23, 24, 42, 72, 74, 75, 77, and 79-82.

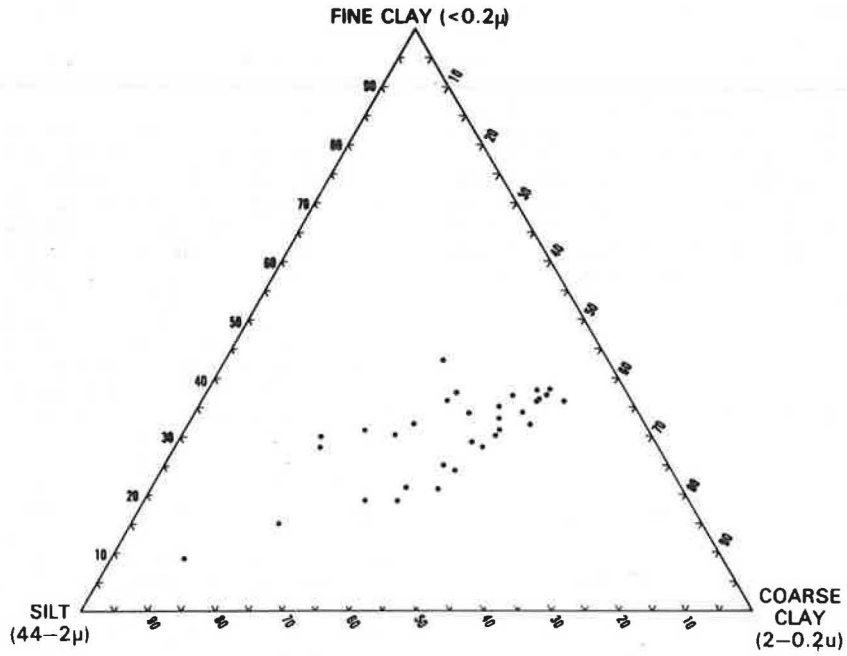

Figure 5. Relative proportions of clay minerals (quartz and feldspars) and carbonates in red clay.

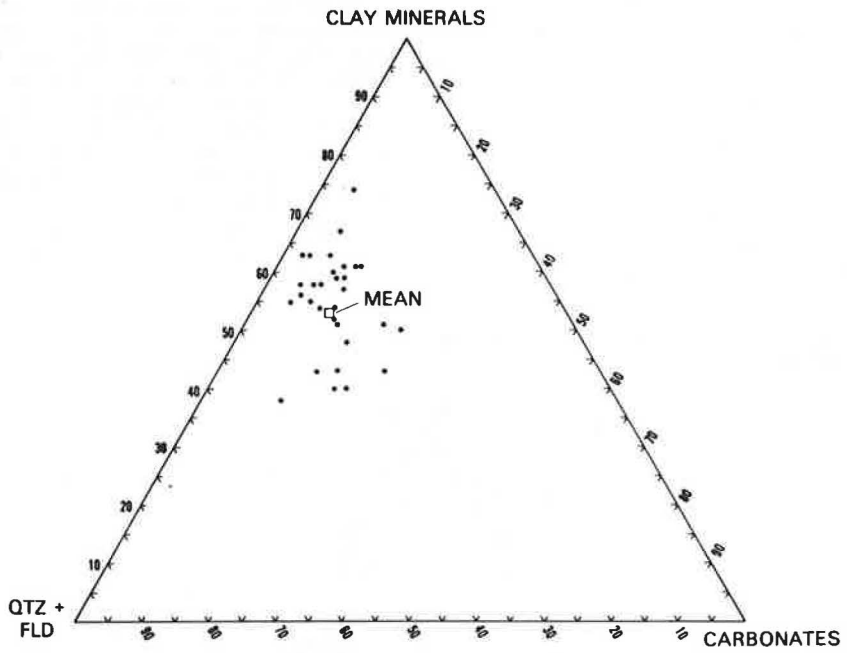

tionship between the mineral content of a separated fraction and the size range of the separate. This relationship is shown in Figures 7 and 8. Figure 7 contains cumulative curves where each component considered (quartz, feldspar, carbonates, whole sample) is normalized to 100 percent and its cumulative distribution is plotted versus the logarithmic phi scale. As expected, the nonclay minerals are coarser than the red clay as a whole. When the derivatives of these cumulative curves are plotted in Figure 8 (percent phi/phi unit versus phi), all of the nonclay minerals peak in the region of 9 phi (μm). Carbonate has a high differential peak because there is little carbonate in the sand or clay fraction so the cumulative curve for carbonate (Figure 7) rises very fast in the silt range. The high proportion of primary minerals in the size range 90 to 120 (2 to 0.2 μ) is indicative of the glacial rock flour component of the red clay and of the lack of weathering attack on the material.

The distribution of clay mineral species as a function of particle size is given in Table 2 where the percentage of illite in silt plus the percentage of illite in coarse clay plus the percentage of illite in fine clay is set to 100 percent, and the same is done for smectite and chlorite. These nor-

Figure 6. Relative proportions of smectite, illite, and chlorite in fine clay (<0.2 μm) fraction.

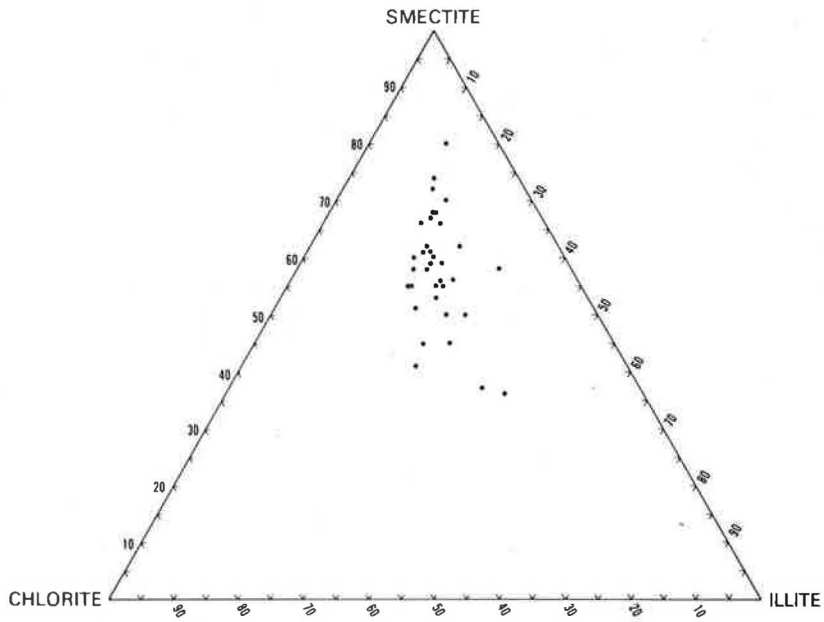

Figure 7. Cumulative curves for mineral species in red clay.

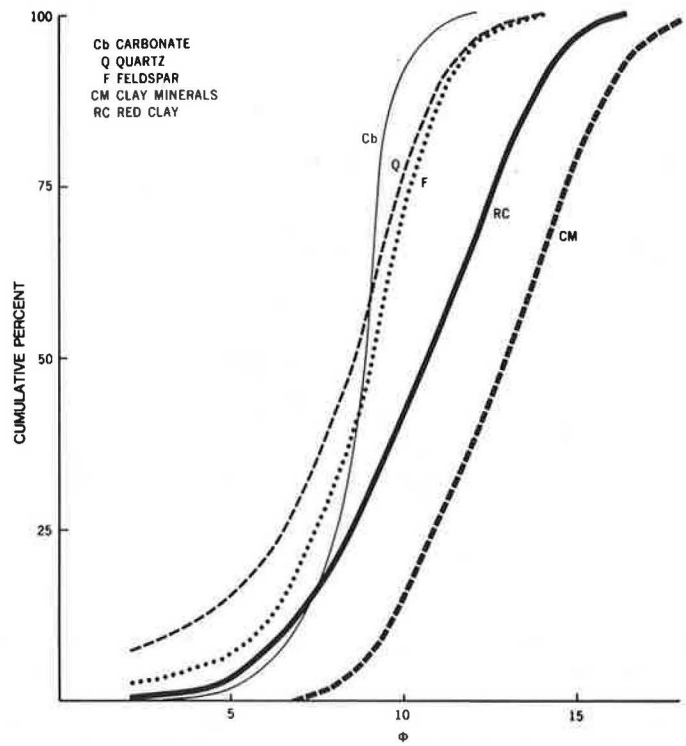

Table 1. Average percentage of components of red clay derived from the boreholes shown in Figure 2.

Size Fraction	Weight Percent Size Fraction	Quartz	Potassium Feldspar	Plagio-clase Feldspar	Calcite	Dolomite	Smectite	Illite	Chlorite	Total
>44 μm	4 (4)[a]	60 (5)	24 (10)	14 (5)	2 (1)	2 (1)	–	–	–	102
44 to 2 μm	24 (12)	34 (4)	15 (4)	14 (4)	7 (5)	15 (5)	2 (2)	5 (2)	8 (4)	100
2 to 0.2 μm	42 (7)	19 (5)	13 (4)	10 (4)	5 (5)	6 (3)	9 (3)	13 (4)	25 (4)	101
<0.2 μm	30 (6)	–	–	–	–	–	60 (7)	19 (4)	20 (5)	99
Weighted sum	100	19	10	8	4	6	22	12	18	99

[a]Values in parentheses are standard deviations.

Table 2. Normalization of clay mineral contents so that each species sums to 100 percent: cumulative results.

Mineral Species	Size Fraction	Average Percent of Mineral in Separate	Average Weight Fraction of Separate	Percent in Whole Clay[a]	Normalized Clay Percent	Cumulative Sum of Clay Species
Smectite	Silt	2.4	0.256	0.61	2.8	2.8
Smectite	Coarse clay	9.0	0.398	3.58	16.3	19.1
Smectite	Fine clay	61.8	0.288	17.8	80.9	100.0
Illite	Silt	4.6	0.256	1.18	10.7	10.7
Illite	Coarse clay	11.4	0.398	4.54	41.1	51.8
Illite	Fine clay	18.5	0.288	5.33	48.2	100.0
Chlorite	Silt	7.1	0.256	1.82	10.7	10.7
Chlorite	Coarse clay	23.8	0.398	9.47	55.8	66.5
Chlorite	Fine clay	19.7	0.288	5.67	33.4	100.0

[a]Product of average percent of mineral in separate and average weight fraction of separate.

Figure 8. Curves derived from Figure 7.

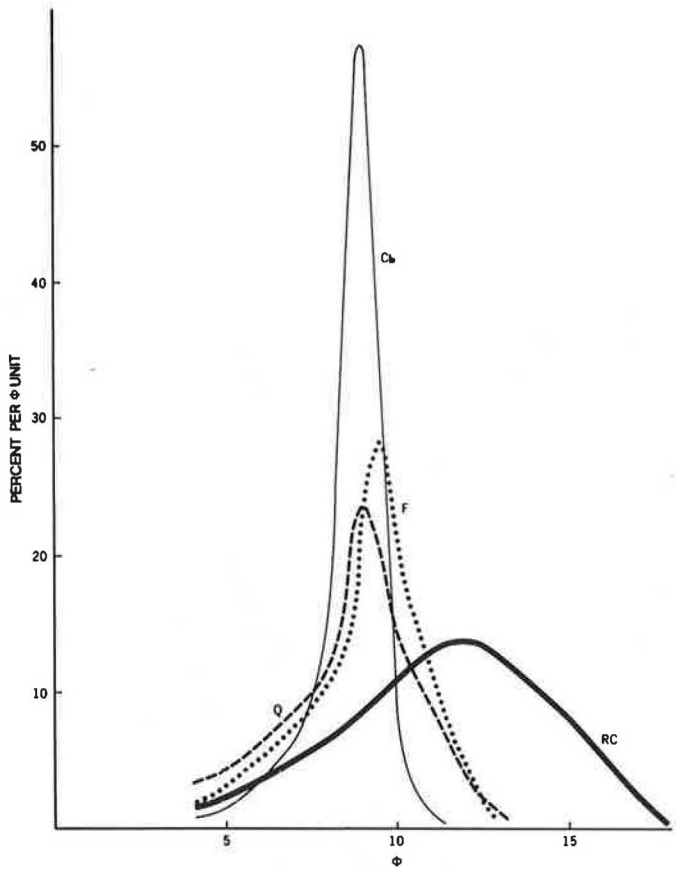

malized values show that more than 80 percent of the smectite occurs in the fraction finer than 0.2 μm, and more than 50 percent of the illite and chlorite occurs in the silt and coarse clay fractions. This suggests that the shrink-swell behavior of the red clay is closely related to the amount of <0.2 μm clay. However, the Atterberg limit values correlate no more strongly with the percentage <0.2 μm clay than with the <2 μm clay.

CORRELATION OF ATTERBERG LIMIT DATA WITH MINERALOGICAL AND SIZE DISTRIBUTION DATA

The data distribution shown in Figure 9, a plot of liquid limit versus plasticity index, is another indication of the mineralogic uniformity of the red clay (represented by points in the figure). Casagrande (4) has shown that sample groups following the A line come from soils having mineralogic uniformity.

Figures 10 and 11 show the relationship of the plasticity index (PI) values and the liquid limit (LL) values to the content of <2 μm clay (circled values are not included in the regression calculation). This relationship defines "activity" (5, p. 107). A least squares fit of a straight line to these two data clusters generates the following equations.

$$PI = -0.1 + 0.51\ (\% < 2\ \mu m\ clay) \quad r = 0.84,\ s_{y.x} = 3.0 \tag{1}$$

$$LL = 10.0 + 0.78\ (\% < 2\ \mu m\ clay) \quad r = 0.76,\ s_{y.x} = 5.8 \tag{2}$$

$$PI = 0.65\ LL - 6.6 \tag{3}$$

Figure 9. Plasticity index versus liquid limit.

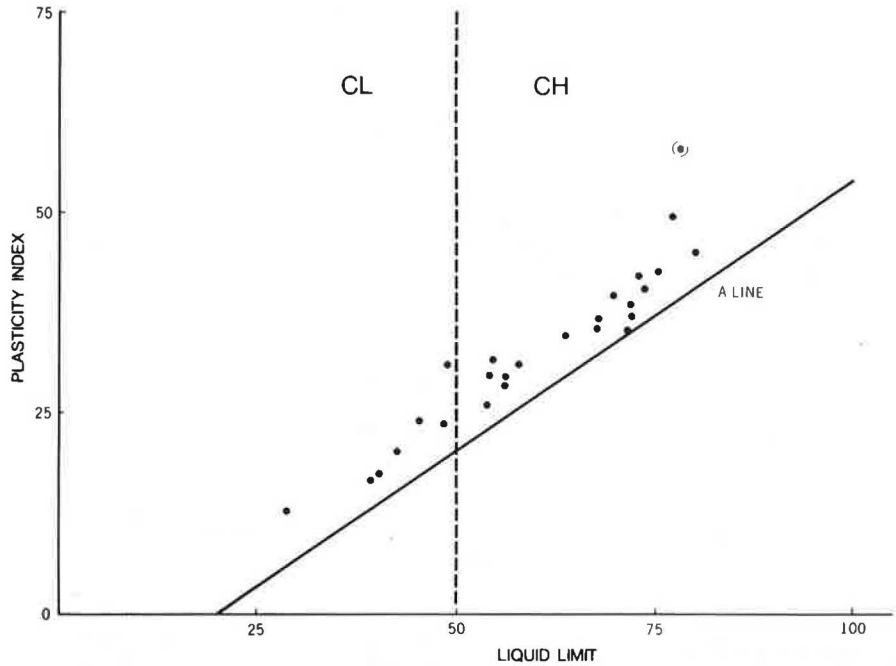

Figure 10. Plasticity index versus percent <2 μm clay.

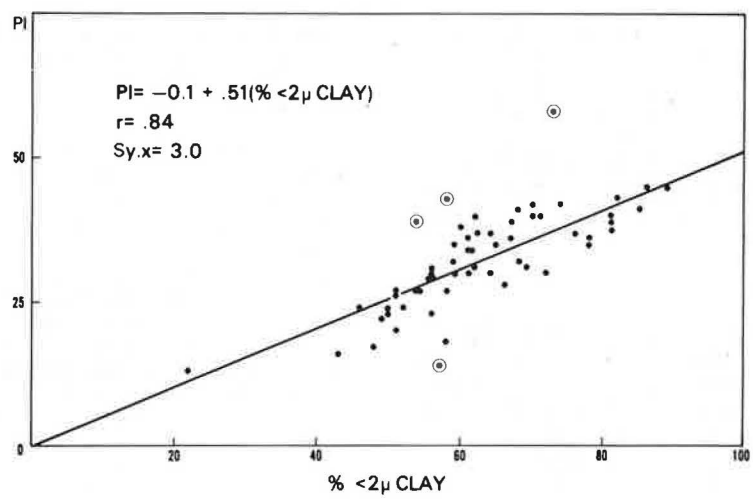

The slope of the line (activity) for Equation 1 falls about midway between accepted values (5) for illite clays (activity = 0.9) and kaolinite clays (activity = 0.3). This clay contains significant smectite which, when pure, can give rise to very high activities (1.5 or more). The <2 μm fraction contains, on the average, about one-third minerals (quartz, feldspars, carbonates), one-third chlorite + illite, and one-third smectite. This distribution will produce a slope in the vicinity of 0.7 if chlorite is assumed to be like kaolinite and the primary minerals are assumed to have zero slope. The observed slope of 0.51 is therefore lower than what would be predicted on the basis of mineral content.

Equation 2 relating LL to % <2 μm clay is combined with Equation 1 to give the relationship between plasticity index and liquid limit. The parameter N (0.65) is in reasonable agreement with the value from Seed et al. (5) for a clay with 0.5 activity.

Angle of Internal Friction

Undrained triaxial shear tests run at a slow rate (6 hours to obtain failure) on three sets of core samples taken in the NE1/4 sec. 36, T. 49 N., R. 14 W. provide the best data currently available from which values of internal friction angles (0 angles) and cohesion can be obtained (Table 3). Construction site data give internal friction angles ranging from a low of 11 degrees to a high of 32 degrees. Present data suggest that an internal friction angle of about 18 to 20 degrees for the effective state is reasonable. Based on long-term natural slope angles, an internal friction angle about half as great is

Figure 11. Liquid limits versus percent <2 μm clay.

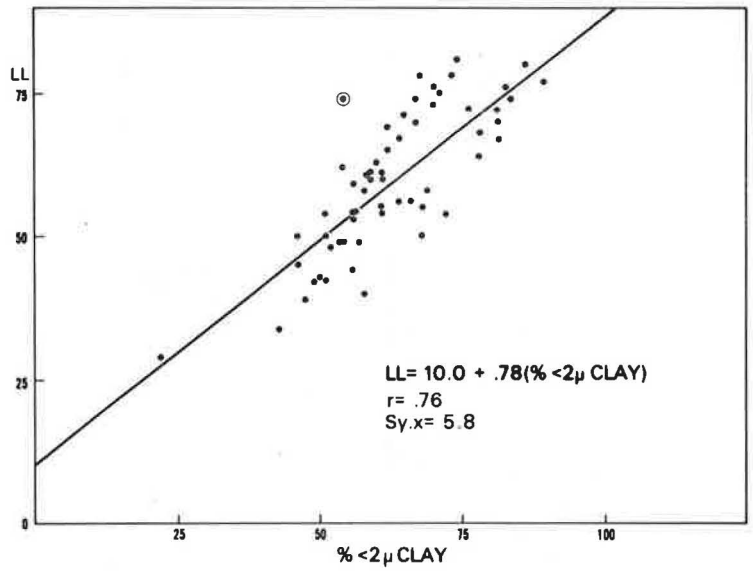

Table 3. Cohesion and angles of internal friction of three cores (NW1/4 sec. 36, T. 49 N., R. 14 W).

	Angle of Internal Friction		
Depth (ft)	Total Stress	Effective Stress	Cohesion
12 to 14	12.5	17.0	0.05 kg/cm^2
32 to 35	9.0	14.0	0.20 kg/cm^2
80 to 82	8.5	9.5	0.35 kg/cm^2

indicated for the total stress state. More study is needed to establish regional variations in materials and to associate internal friction angles with particular stratigraphic units.

SLOPE FAILURE IN RED CLAY

An important failure mode, which has been observed in the red clay material and studied in the valley of Little Balsam Creek (tributary to the Nemadjii River) (6), involves (a) loss of toe support at the valley bottom, (b) surficial cracking of the clay, and (c) sliding of blocks of clay material as on a decollement surface. Factors that appear to favor such failure include (a) smectite-rich clay with substantial shrink-swell capacity, (b) decreased infiltration and greater runoff in recent times with consequent rapid stream erosion, due perhaps to logging and agricultural practices, and (c) a possible increase in surficial drying of the clay since the cutting of the climax forest.

Cracking of these soils during the growing season is well known (1, p. 114). Such behavior is not unlike that of soil order Vertisol (8, p. 375). Vertisol soils are smectite-rich soils that develop in climates with a pronounced dry season and that cause problems for construction and agriculture even on the flat. Logging operations of the past century may have exacerbated the cracking behavior and contributed to the rate of slope failure. This possibility can still be examined; Hole (7, p. 114) reports virgin soils (Ontonagon series) under two-century-old white pine trees on Madeline Island of the Apostle group. Cracking behavior of virgin and cultivated soils can still be compared.

Cracking apparently contributes to slope failure by providing conduits that rapidly transmit water to the base of the cracked zone. In this zone a subsurface layer, which is a layer of weakness due to its higher moisture content, develops. This weak zone promotes decollement-sheet-like sliding of the surficial blocks. This type of failure is particularly evident on slopes that average 15 to 18 degrees toe to crest, and such slopes are common on drainage ways in the red clay region.

CONCLUSIONS

Most of the highly active clay (smectite) is in the <0.2-μm fraction, yet the Atterberg limit values correlate no more strongly with the 0.2-μm fraction than with the <2-μm clay.

The <2 μm fraction contains about one-third primary minerals, one-third less-active clay minerals (chlorite and illite), and one-third active clay (smectite). This distribution will produce an activity in the vicinity of 0.7 if chlorite is assumed to be like kaolinite and the primary minerals are assumed to have zero slope. The observed activity of 0.5 is therefore lower than would be predicted based on the sums of the mineral contents.

An internal friction angle of about 18 to 20 degrees for the effective state is a reasonable assumption. Long-term natural slope angles indicate an internal friction angle about half as great.

Slope failure in stream valleys frequently takes the form of a cracked surficial layer sliding on a more plastic substratum.

ACKNOWLEDGMENT

This work was supported by U.S. Environmental Protection Agency grant No. G-005140-01. We wish to thank the Douglas County Highway Department and Emil Meintzner whose crew and equipment were necessary for sample collection and who ran the Atterberg limits on the samples.

REFERENCES

1. R.W. Farrand. The Quaternary History of Lake Superior. Proc. Twelfth Conference of Great Lakes Research, International Association for Great Lakes Research, 1969, pp. 181-197.
2. M.L. Jackson. Soil Chemical Analysis: Advanced

Course. Privately printed, Madison, Wis., 1956.
3. N.V. Aquilers and M.L. Jackson. Iron Oxide Removal from Soils and Clays. Proc. 17 of the Soil Science Society of America, 1973, pp. 359-364.
4. A. Casagrande. The Determination of Pre-consolidation Load and its Practical Significance. Proc., First International Conference on Soil Mechanics and Foundations, 1936.
5. H.B. Seed, R.J. Woodward, Jr., and R. Lundgren. Clay Mineralogical Aspects of the Atterberg Limits. Journal of Soil Mechanics and Foundations Division, ASCE, Vol. 90, No. SM4, 1964.
6. J.T. Mengel, Jr., and B.E. Brown. Red Clay Slope Stability Factors. Wisconsin Department of Transportation, District 8; U.S. Environmental Protection Agency, Final Rept., 1976.
7. F.J. Hole. Soils of Wisconsin. Univ. of Wisconsin Press, Madison, Wis., 1976.
8. Soil Taxonomy. Soil Conservation Service, U.S. Department of Agriculture, 1975.

Publication of this paper sponsored by Committee on Soil and Rock Properties.

Geotechnical Evaluation of Loessial Soils in Kansas

S.S. BANDYOPADHYAY

Much of western, central, and northeastern Kansas is covered with loess deposits from Bignell, Peoria, and Loveland formations along with Sangamon soils above Loveland unit. In this paper their significant geological and engineering properties are defined, and design guidelines are presented. Montmorillonite is the chief cementing agent in Kansas loess. The Sangamon soil and the Loveland loess contain more clay than the Bignell loess and the Peoria loess and have higher in situ density and less permeability. The in situ density of Bignell loess and Peoria loess is less than 85 pcf, and consolidation tests and field experience indicate that they are highly susceptible to hydroconsolidation. A key factor in the collapse potential of Kansas loessial soils appears to be the mineralogy of the soils, specifically the presence of montmorillonite as the chief cementing agent; montmorillonite has the ability to adsorb more hydrogen cations than kaolinite and thus is able to adsorb more water. Total stress parameters must be used to design loess slopes approaching the vertical, and effective stress methods are particularly applicable in dealing with saturated loess and with seepage stresses where flattened slopes are required. Saturated loess may liquefy due to the cyclic nature of earthquake loading. Stabilization and compaction of loess represent not only an antisubsidence but also an antiliquefaction measure. Proper consideration should be given to zoning of areas of collapsible loessial soils.

Loess, a wind-deposited soil composed predominantly of silt-sized particles, is found in western, central, and northeastern Kansas. Loess is also found in approximately 17 percent of the United States, 17 percent of Europe, 15 percent of Russia and Siberia, and large areas of China as well as in New Zealand and the plains region of Argentina and Uruguay. Loess appears to be formed by wind-borne deposits traveling over glacial outwash with the higher humidity of the outwash causing precipitation of the soil particles. The geotechnical properties of loess deposits and their unique characteristics are of special practical importance to the geotechnical engineer, as well as to the agriculturist. Even though Terzaghi (1) described the properties of loess as "international" when comparing the data presented by Scheidig (2) and Holtz and Gibbs (3), Peck and Ireland (4) regarded loess "not as a soil of remarkably constant and uniform properties, but as one possessing local and regional variations almost as striking as those of some glacial materials."

Present foundation and earthwork design procedures, used in connection with this incompletely understood deposit, are still nearly all empirically based. The purpose of this paper is to define the significant geologic and engineering properties of Kansas loessial soils, to identify the potential geotechnical problems associated with them, and to present design guidelines related to these soils. Data from numerous open project files of the Kansas Department of Transportation have been used in developing this paper as well as material from a variety of published reports.

GEOLOGY

The major sources of loessial soils in Kansas are the Platte River valley of western Nebraska, the Missouri River valley, and the Republican River valley. The deposition of silts from these sources is generally attributed to eolian action. The stratigraphy of the major loess members and associated Pleistocene strata in Kansas is shown in Figure 1.

Bignell Member

Significant deposits of Bignell, the youngest of the major loess units, have been found in northwestern (thin and discontinuous) and northeastern (Missouri River valley bluffs in Doniphan County) Kansas. Bignell loess is so similar to Peoria loess that they can hardly be distinguished unless the Brady soil occurs stratigraphically below it (5). The Brady soil was formed during a short interglacial interval known as the Bradyan substage. The Brady profile is moderately to poorly drained and the depth of leaching ranges from 1 to 3 feet. Molluscan fauna fossils are sometimes contained within the Bignell loess.

Peoria Member

Typically yellow-tan in color, the Peoria loess occurs predominantly in Kansas and was deposited during the interval between the Iowan and Mankato glacial substages in Iowa. The deposition of the Peoria loess may have occurred during the relatively dry cycle following the melting of the ice sheet. The Peoria member ranges in texture from a very fine